data suggested a better comfort for the patient for linac-based therapy, due to the shorter treatment time and the non-invasive immobilization system. Dosimetric data for the patients treated according to this protocol suggest a substantial balance between Gamma Knife and Linac EDGE treatments

Poster: Physics track: (Radio)biological modelling

PO-0870

Fitting data of relapse-free survival after post-prostatectomy RT with a comprehensive TCP model

C. Fiorino[1], S. Broggi[1], N. Fossati[2], C. Cozzarini[3], G. Goldner[4], T. Wiegel[5], W. Hinkelbein[6], J.R. Karnes[7], S.A. Boorjian[7], K. Haustermans[8], S. Joniau[9], S. Shariat[10], F. Montorsi[11], H. Van Poppel[9], N.G. Di Muzio[3], R. Calandrino[1], A. Briganti[2]
[1]*San Raffaele Scientific Institute, Medical Physics, Milano, Italy*
[2]*San Raffaele Scientific Institute, Division of Oncology/Unit of Urology, Milano, Italy*
[3]*San Raffaele Scientific Institute, Radiotherapy, Milano, Italy*
[4]*Medizinische Universitat Wien, Klinik fur Radioonkolgie, Wien, Austria*
[5]*University Hospital Ulm, Department of Radiation Oncology, Ulm, Germany*
[6]*Charitè Universitats Medizin- Campus Benjamin Franklin, Department of Radiation Oncology, Berlin, Germany*
[7]*Mayo Clinic Rochester, Department of Urology, Rochester, USA*
[8]*University Hospital Leuven, Department of Radiotherapy, Leuven, Belgium*
[9]*University Hospital Leuven, Department of Urology, Leuven, Belgium*
[10]*Medical University of Vienna- Vienna General Hospital, Department of Urology, Wien, Austria*
[11]*San Raffaele Scientific Institute, Department of Oncology/Unit of Urology, Milano, Italy*

Purpose or Objective: By pooling data of five large prospective studies/Institutional series, a large data base of pT2-pT3, pN0 patients treated either in the adjuvant or in the salvage setting with conventionally fractionated (1.8-2.0 Gy/fr) 3DCRT post-prostatectomy radiotherapy (RT) was available. The aim of the study was to fit individual data of biochemical-recurrence-free survival (bRFS) with a comprehensive Poisson-based TCP model.

Material and Methods: Considering pre-RT PSA as a surrogate of the number of clonogens, 5-year bRFS was expressed as a function of the dose depending on radiosensitivity (α_eff), number of clonogens for pre-RT PSA=1ng/mL (C) and the fraction of patients that relapses due to clonogens outside the treated volume, assumed to linearly depend on pre-RT PSA (K=1-BxPSA), according to:
bRFS = (1-B x PSA) x [1 - exp (-α_eff D)]^CxPSA.
In addition, the impact of Gleason score (GS) was included by performing separate fits for different sub-groups, depending on GS (<7,=7,>7). In total, complete data regarding bRFS, dose, pre-RT PSA (between 0.01 and 2.0 ng/ml) and GS of 894 hormono-naive patients treated with adjuvant (n=331) or salvage (n=563) intent with a minimum follow-up of 3 years were available. Patients with GS<7, =7 and >7 were 392, 383, and 119 respectively. Best-fit procedures were performed with the sequential quadratic programming, using the sum of the squared residuals error as loss function (SPSS v.17, SPSS Inc., Chicago, IL). The 95% CI of the parameter's best-fit values were calculated by bootstrap. The performance of the resulting model was assessed by calibration plot.

Results: The median follow-up was 72 months; median pre-RT PSA and dose were 0.25 ng/mL (inter-quartile range: 0.1-0.5) and 66.6Gy (range:59.4-77.4Gy) respectively. The fit converged in all situations: depending on GS, best-fit values were in the range 0.20-0.22 Gy-1 and 10^6 for α_eff and C respectively; the maximum obtainable bRFS was reduced by 1.7, 4.9 and 5.6% for each 0.1ng/ml PSA increment for GS<7, =7 and >7 respectively. The calibration plot showed an excellent agreement between predicted and expected values (R2=0.96) and the AUC was 0.69 (95% CI: 0.66-0.73). The bRFS curves as estimated by the model vs prescribed dose for different pre-RT PSA (between 0.1 and 1.0 ng/ml) and for the three GS groups are plotted in the figure.

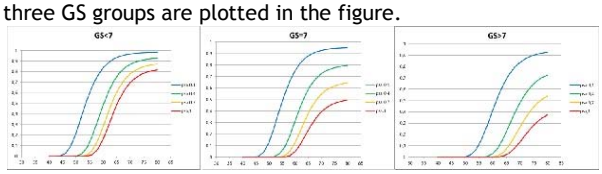

Conclusion: Long-term bRFS data of a large multi-centric data base of post-prostatectomy patients could be fitted by a radiobiologically consistent TCP model, showing a dose-effect critically depending on pre-RT PSA and GS. The model suggests that most relapses occur in patients with clonogens outside the treated volume, indirectly supporting lymph-nodal irradiation and/or systemic therapy for specific risk groups, depending on pre-RT PSA and GS. Early RT is preferred over delayed RT as the detrimental effect due to a PSA increase can never be compensated by increasing the dose, more dramatically evident for patients with GS ≥7.

PO-0871

Radiation-induced lung damage: beyond dose-volume histogram analysis

S. Monti[1], G. Palma[2], V. D'Avino[2], M. Conson[3], R. Liuzzi[2], M.C. Pressello[4], V. Donato[5], J.O. Deasy[6], R. Pacelli[3], L. Cella[2]
[1]*IRCCS SDN, Naples, Italy*
[2]*National Research Council, Institute of Biostructure and Bioimaging, Naples, Italy*
[3]*Federico II University School of Medicine, Department of Advanced Biomedical Sciences, Naples, Italy*
[4]*S. Camillo-Forlanini Hospital, Department of Health Physics, Rome, Italy*
[5]*S. Camillo-Forlanini Hospital, Department of Radiation Oncology, Rome, Italy*
[6]*Memorial Sloan Kettering Cancer Center, Department of Medical Physics, New York, USA*

Purpose or Objective: Traditional normal tissue complication probability (NTCP) models rely on dose-volume histogram (DVH) analysis, which disregards any spatial dose distribution information and possible inhomogeneity in regional organ radio-sensitivity. We propose a voxel-based (VB) approach to correlate local lung dose and radiation-induced lung damage (RILD).

Material and Methods: An inter-institutional database of 115 Hodgkin lymphoma survivors treated with sequential chemo-radiotherapy (with 18 RILD cases after treatment) were included in the study. Sixteen patients were excluded due to an inadequate CT coverage of the lungs.
Each patient dataset was first normalized to a common template. Pre-registration steps were based on a binary mask extrapolated from the organ at risk segmentations of the treatment plan. For each patient, the mask, computed as the union and dilation (spherical structuring element of radius 30 mm) of heart and lung structures, was used to crop the field-of-view, allowing a coarse alignment of the structures of interest. CT images were masked accordingly in order to hide some anatomical inter-individual differences, and allowed the registration algorithm to work more efficiently on tissue contrast inside the chest. The median lung-volume patient was chosen as reference image in the non-rigid registration and a log-diffeomorphic approach [1] was used. The obtained deformation fields were then used to map the dose of each patient to the common coordinate system of the reference patient.
A voxel-wise two-sample t-test was then performed on the normalized dose maps and statistically significance of the differences between groups was displayed as p-value map.

Results: The robustness of co-registration process was assessed both by visual inspection (Fig. 1a-b) and by Dice scores for the lungs (Fig. 1c). On the whole population, the median Dice value was 0.94 (range: [0.87; 0.95]). As shown in

Fig. 1d-f, a significantly ($p < 0.01$) higher dose was delivered to RILD patients nearby the basal portion of the right lung and the submantellar region of the left lung. The average dose delivered to this volume (9.4% of the lungs) was of 5.3 Gy in RILD patients and 2.6 Gy in non-RILD patients.

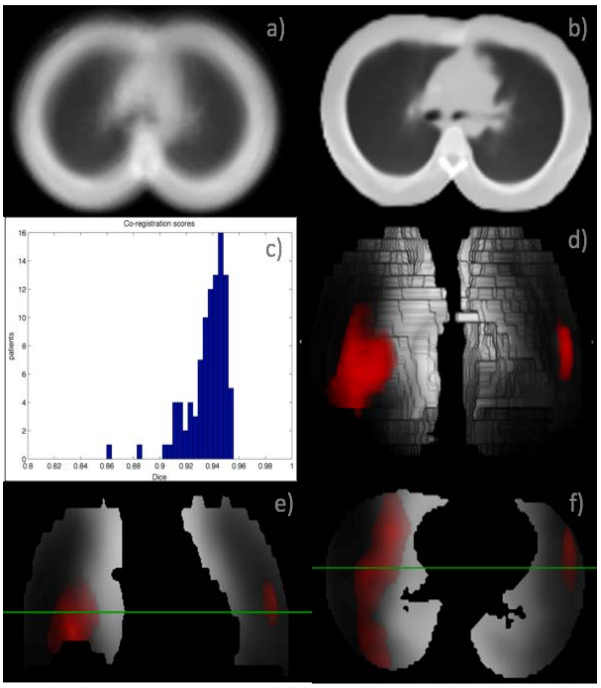

Figure 1. a) Average of the pre-registration CTs. b) Average of the post-registration CTs. c) Lung Dice scores distribution. d) 3D anteroposterior volume rendering of the mean RILD patients' dose (gray scale) with in red the *p*-value map (masked for $p < 0.01$). e) Coronal view of the mean RILD patients' dose (gray scale) with in red the *p*-value map (masked for $p < 0.01$). f) Axial view of the mean RILD patients' dose (gray scale) with in red the *p*-value map (masked for $p < 0.01$).

Conclusion: By a VB approach we were able to highlight local dose-RILD relationship in the lungs. Interestingly, a significantly different dose was delivered in the low-dose (~ 5 Gy) parenchymal regions, in agreement with previous DVH analyses showing that the volume exceeding 5 Gy is consistently more predictive than other dosimetric variables.
In order to obtain more powerful insights on local lung radiosensitivity, this preliminary results should be enriched by applying the VB approach to larger databases evaluating RILF in heterogeneously treated lungs.

[1] Vercauteren T, Pennec X, Perchant A, Ayache N. Symmetric log-domain Diffeomorphic registration: A demons-based approach. In lecture notes in computer science: Vol 5241. MICCAI 2008

PO-0872

The variability of the RBE in proton therapy: can we base it on empirical clinical data?

A. Lühr[1,2,3], C. Von Neubeck[1,2,3], M. Baumann[1,2,3,4,5], M. Krause[1,2,3,4,5]

[1]*German Cancer Consortium DKTK, Partner Site Dresden, Dresden, Germany*
[2]*OncoRay - National Center for Radiation Research in Oncology, Faculty of Medicine and University Hospital Carl Gustav Carus- Technische Universität Dresen- Helmholtz-Zentrum Dresden-Rossendorf, Dresden, Germany*
[3]*German Cancer Research Center DKFZ, Heidelberg, Germany*
[4]*University Hospital Carl Gustav Carus- Technische Universität Dresden, Department of Radiation Oncology, Dresden, Germany*
[5]*Helmholtz-Zentrum Dresden - Rossendorf, Institute of Radiooncology, Dresden, Germany*

Purpose or Objective: Particle therapy has the potential to improve radiotherapy due to the increase in dose conformity and RBE. The RBE depends on multiple factors including cell type, dose, particle type and energy. Accordingly, a variable RBE is clinically applied for carbon ion therapy, in contrast to a prescribed constant RBE = 1.1 in proton therapy jeopardizing part of its accuracy. Therefore, it is the aim to enhance proton therapy by translating a more realistic RBE description into the clinic directly based on clinical (and preclinical) experience gained with photons and heavier ions such as helium and carbon ions.

Material and Methods: The RBE is considered to depend on a) the dose response of the biological endpoint and b) the heterogeneity of the dose distribution on the cellular level (similar to the local effect model). The heterogeneity is determined by the clinically accessible (prescribed) dose D and the beam quality $Q = Z^2/E$ (varying within the patient), where Z and E are the ion charge and kinetic energy, respectively. We propose an approach to obtain proton RBE by interpolating between the biological effectiveness of a homogeneous dose distribution for photons and an increasingly heterogeneous distribution for heavier and slower ions. Based on the linear-quadratic (LQ) model and the dose heterogeneity an analytical description of the radiobiological effect was derived. It suggests a linear increase of the LQ parameter for particle irradiation αP with beam quality Q. *In vitro* RBE data from the literature for different ion types, cell lines, and within clinically relevant LET ranges (below the RBE maximum) were analyzed.

Results: The considered RBE data seem to depend directly on beam quality Q (Figure 1a). In contrast, particle type together with LET appear as a surrogate for beam quality Q (Figure 1b). In accordance with the derived description, the LQ parameter αP increases linearly with Q (Figure 1c) and the RBE (Figure 1d) as well as αP could be approximated for all considered ions and cell lines with a simple formula depending on Q, D, and the photon LQ parameters αX and βX. The deviations between prediction and experiment are mostly within 10 - 20% and therefore on the order of uncertainties often associated with RBE experiments. The variation of βP with Q was much weaker and less conclusive.

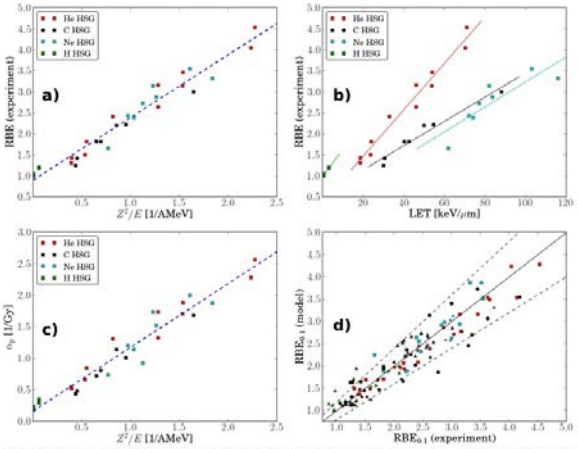

Figure 1: Biological effectiveness for different beam qualities, beam energies, and ion types: green, proton; red, helium; black, carbon; cyan, neon. The same in vitro RBE data for human salivary gland tumor (HSG) cells as a function of a) beam quality $Q = Z^2/E$ and b) LET. c) Linear LQ parameter as function of Q for HSG cells. d) Modeled compared to measured RBE values for about 125 different combinations of cells, ion types and energies. The dashed lines visualize a 20% spread around the solid identity line. All lines are just to guide the eye.

Conclusion: As long as cells "experience" a comparable microscopic dose distribution they cannot distinguish between different ion beams confirming that RBE variability also exists in proton therapy. More realistic RBE values for proton therapy may be directly obtained from available empirical RBE data for heavier ions considering the same beam quality Q and endpoint or, alternatively, by interpolating between empirical data from photon irradiation and heavier ions. Experimental preclinical (and clinical) data should be gathered in order to validate the proposed strategy to enhance proton therapy.